Optimal Topology-Aware PV Panel Floorplanning with Hybrid Orientation

Optimal Topology-Aware PV Panel Floorplanning with Hybrid Orientation

Sara Vinco
Politecnico di Torino
Torino, Italy 10129
sara.vinco@polito.it

Enrico Macii
Politecnico di Torino
Torino, Italy 10129
enrico.macii@polito.it

Massimo Poncino
Politecnico di Torino
Torino, Italy 10129
massimo.poncino@polito.it

ABSTRACT

Despite of being one of the most widespread green energy sources, the efficiency of PV rooftop installations is still repressed by shading and by the absence of a rigorous irradiance-aware placement approach. The goal of this work is to reach optimal energy production via an irregular placement of PV modules, by considering two degrees of freedom: *orientation* of each PV module and *topology*. Experimental results will prove the effectiveness of the proposed solution onto two real world case studies, with an increase of power production of up to 40%.

KEYWORDS

Power Optimization; Renewable Energies; PV panels

ACM Reference format:
Sara Vinco, Enrico Macii, and Massimo Poncino. 2018. Optimal Topology-Aware PV Panel Floorplanning with Hybrid Orientation. In *Proceedings of 2018 Great Lakes Symposium on VLSI, Chicago, IL, USA, May 23--25, 2018 (GLSVLSI '18),* 4 pages.
https://doi.org/10.1145/3194554.3194646

1 INTRODUCTION

The placement of a PV installation is a critical step in its deployment: in order to maximize the return on investment, it is essential to find locations with maximum solar irradiance and minimal or zero shading. For an optimal placement, meteorological information are therefore essential. The literature on the placement of PV installations mostly deals with the positioning of the PV array *as a whole*, while the modules composing the array are all laid out using the same orientation (portrait, more typically, or landscape) without any apparent reason other than ease of connection.
Moreover, topological information is typically not exploited by traditional placements, despite of its impact on the final power production, as it could help matching the variance in irradiance on the surface and minimize the effects of shading. Therefore, thinking in terms of the PV panel as a whole, without any freedom in the orientation and the interconnection of the individual modules, may result in a sub-optimal power production.

GLSVLSI '18, May 23--25, 2018, Chicago, IL, USA

ACM ISBN 978-1-4503-5724-1/18/05…$15.00
https://doi.org/10.1145/3194554.3194646

Clearly, in order to constructively build such a topology-aware placement allowing also hybrid orientation, we need *fine-grain environmental data*, in terms of both spatial and time resolution. Although many Geographic Information Systems (GIS)-based tools are available [2, 5, 7, 9], the only one with the desired spatial and temporal resolution is the one described in [1], which we will adopt as the underlying source of environmental data.
Concerning related approaches, some works leverage finer-grain GIS solar data to drive PV installations at a smaller scale, but in most cases they are just used to identify suitable surfaces (roofs) for the installation. Only few works (e.g. [15]) use fine-grain solar data to identify the best position of PV panels on rooftops; however, they provide only qualitative feedback.
In this work, we specifically address the issue of the *optimal placement of a solar panel on a rooftop based on fine-grain GIS data*. Our method, given a set of irradiance data, a target area for the placement and the topological information of the panel, determines a tiling of the entire surface with a number of PV modules that maximizes the total extracted power. Results show that the determined placement can extract 12-42% more energy than a traditional placement, depending on the target roof, the placement used as a reference, and the adopted PV model.

2 BACKGROUND AND MOTIVATION

2.1 Background

A photovoltaic cell is described by a voltage-current (I-V) characteristic curve, which plots, at a given temperature, the variation of I as a function of the irradiance G [11]. As G increases, the open-circuit voltage V_{oc} increases logarithmically and the short-circuit current I_{sc} increases proportionally. At a given irradiance G, a temperature increase yields a slight increase of the short-circuit current I_{sc}, which determines a decrease of V_{oc}.
In order to increase the output power, cells are connected together according to a series/parallel organization into a PV *module*. PV modules can be further interconnected together. Given n parallel strings each of m modules in series, the total power is obtained as $P_{panel} = V_{panel} \cdot I_{panel}$, where:

$$\begin{cases} V_{panel} = \min_{j=1,\ldots,n}(\sum_{i=1,\ldots,m} V_{module,ij}) \\ I_{panel} = \sum_{j=1,\ldots,n}(\min_{i=1,\ldots,m} I_{module,ij}) \end{cases} \quad (1)$$

and $V_{module,ij}$ and $I_{module,ij}$ are the voltage and the current extracted from the i-th module in the j-th string. The above formulas show that the total power extracted by the panel P_{panel} depends on its topology and is generally different from the sum of the power of the individual modules, since a non uniform irradiance, e.g., as an effect of shading, heavily affects the total output power of the PV array.

2.2 Motivation

Rooftop PV panels are typically placed by avoiding as much as possible visible or potential shadings and by packing them together tightly using either a ''portrait-only'' or a ''landscape-only'' placement style. There is however no technical impediment in using a mix of the two styles: relaxing the constraint of a portrait/landscape only placement could improve the overall extracted power by a better match of irradiance values with respect to the topology.
Orientation of the panels, however, is not the only available degree of freedom. A possibly more powerful option is offered by allowing the connection of non-adjacent modules. Equations 1 highlight indeed that it is convenient to connect modules with similar irradiance (and therefore similar current/voltage levels), in order to minimize the effect of the min() operators.

2.3 Related work

The literature on strategies for the floorplanning of a PV array is quite limited. Some works leverage GIS solar data to drive PV installations, but they generally limit themselves to the identification of suitable surfaces (roofs) for the installation at the urban level.
Only two works use fine-grain solar data to identify the best position of PV panels on rooftops. In [15], the authors provide a qualitative feedback on the portions of a surface that are most suitable for the placement, but they do do not suggest an actual placement. In [12], the authors provide a GIS-based algorithm to place a set of PV modules in such a way that the best match between solar irradiance and modules positions is obtained. In that work, however, it is assumed that the area of the target surface is much larger than the total array surface; the area slack is thus used to generate an irregular (i.e., non rectangular) floorplan. Moreover, the orientation of the modules is kept fixed (specifically, portrait-only).
Our method can be seen as a variant of [12] in which no area slack is provided and both portrait and landscape orientations are allowed.

3 METHOD AND ALGORITHMS

3.1 Problem Definition

The problem we address in this work amounts to the ''tiling'' of a target surface of area A with a number of N rectangular elements (the PV modules), while maximizing an objective function corresponding to the total extracted power. We assume that the area of the surface has also a rectangular size that can exactly contain the N tiles, i.e., $A \equiv N \cdot A_p$, where A_p is the area of a tile.
This problem can generally be reduced to a particular instance of the well-known binning problem called ''domino tiling'' [6, 8], once observed that PV panels de-facto have a 2x1 aspect ratio [4].
We assume the target surface has rectangular size $H \times W$, $H = n \cdot d$, $W = m \cdot d$, where d is the grid squares ($d = \sqrt{A_p/2}$). There are therefore $n \times m$ grid elements (Figure 1-(a)). Each panel of area $A_p = d^2$ covers then two grid squares.
From the grid we generate a bipartite graph $G(V, E, W)$ that is a representation of *possible tiling solutions* (Figure 1-(b)). Each vertex $v \in V$ corresponds to a grid element. Grid nodes are shown with alternating ''colors'' in a checkerboard fashion to denote the partitioning of the set of vertices in two sets. An edge $e_{ij} \in E$ between two

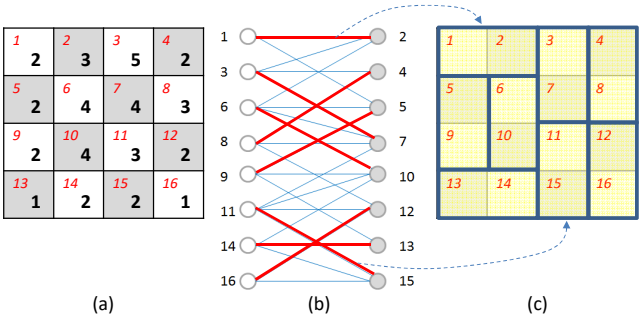

Figure 1: An example 4x4 grid with the relative values (a); the equivalent bipartite graph of the grid (b); an example matching and the corresponding tiling using 2x1 tiles (c).

vertices V_i and V_j exists if they are adjacent in the checkerboard, i.e, they could be covered by a tile.
A *perfect matching* in this bipartite graph represents a tiling of the surface with 2x1 tiles. Figure 1 shows one (randomly chosen) perfect matching (the red edges in Figure 1-(b)) and the corresponding layout of the tiles on the surface (Figure 1-(c)).

3.2 Optimal Tiling Algorithm

This section describes how to derive the weights associated to each grid position and to each edge.
The value assigned to each grid point is a function of the *temporal distribution of irradiance* G, assuming that it is possible to obtain irradiance values at the granularity of our grid cell size d. The average would not be a representative value, since the typical distribution is strongly skewed towards smaller values. As a more aggregate indicator, we therefore use the *75-th percentile of the distribution*, i.e. the value below which 75% of the samples fall (p_{75}). Larger values of the percentile identify distributions that are more skewed towards the upper range of the values; therefore, the suitability metric should combine the percentiles of G, favoring larger values since larger G values are beneficial.
A PV module (tile) covers two grid points, and its cells are typically connected in series. Given that the grid point with the least irradiance will determine the operating point of the whole module, *edge weights* $w_{i,j}$ are simply obtained as $w_{i,j} = \min(p_{75,i}, p_{75,j})$, thus representing the effective irradiance to which the module placed to cover positions i and j will be subject to.
The *maximum matching on the bipartite graph* aims at maximizing these edge weights. We adopted the well-known Hungarian algorithm [10], which in its traditional implementation has a $O(V^4)$ complexity. This is computationally feasible in our case where $|V|$ is in the order of a few tens. The algorithm returns a matching M, which is a subset of the edges (i.e., the red edged is Figure 1.b) and represents the optimal placement of modules (i.e., Figure 1.c).
The next step is to determine the interconnection of the modules according to the specified $s \times p$ topology. This is achieved by using a greedy assignment: we pick edges of M in decreasing order of weight, and assign them in groups of s at a time (a series string). The rationale for this assignment is that it will group modules by guaranteeing a minimal variance of weights w_{ij}, i.e., minimal variance in equivalent irradiance. In this way, the impact of the min() function on the string current (Equation 1) is minimized.

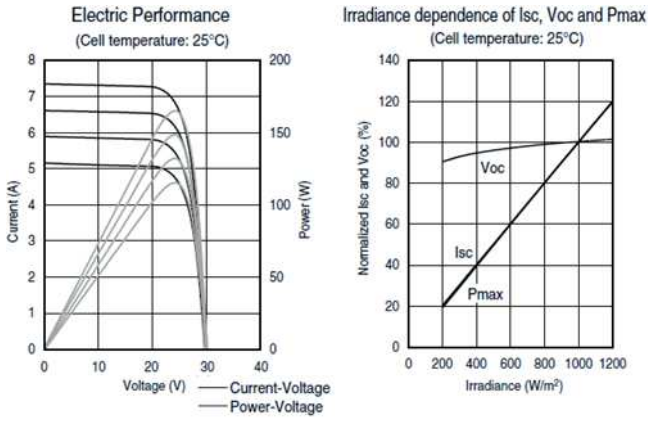

Figure 2: Datasheet of Mitsubishi PV-MF165EB3.

4 EXPERIMENTAL RESULTS

4.1 PV Panel Power Model

In our setup, we consider a PV-MF165EB3 module by Mitsubishi [3]. We adopted a simple PV module model that expresses V_{module} and I_{module} as a function of irradiance G, and we assume that each module extracts the maximum power ($P_{module} \equiv P_{max}$). The model is derived from the plots provided by the datasheet (Figure 2) [13, 14]:

- using the rightmost plot of Figure 2, we first derive the dependence of V_{oc} and P_{max} with respect to irradiance G. The plots are normalized with respect to the reference values at standard condition (25^oC, $1000W/cm^2$) of $V_{oc,ref}$ = 30.4V and $P_{max,ref}$ = 165W, as reported in the datasheet;
- we derive V_{module} from V_{oc} by exploiting the fact that the maximum power voltage of the module is roughly independent of the irradiance and is $\approx$ 80% of V_{oc} (leftmost plot of Figure 2). This allows to express V_{module} as a function of G;
- I_{module} is then derived as the ratio of P_{max} and V_{module}.

This process results in the following equations:

$$V_{oc}(G) = V_{oc,ref} \cdot (0.006105 \cdot G^2 + 1.169 \cdot G + 0.01108)/100$$
$$V_{module}(G) = 0.8 \cdot V_{oc}$$
$$P_{module}(G) = P_{max,ref} \cdot (0.09002 \cdot G - 0.2857)/100$$
$$I_{module}(G) = P_{module}(G)/V_{module}(G)$$

Using then the interconnection rules described in Equations 1, we can derive the voltage V_{panel} and the current I_{panel} of the panel consisting of a $m \times n$ series-parallel interconnection.
Even if the proposed model is relatively simple, the placement algorithm is independent from the adopted PV model, and it thus can be easily extended to more accurate models.

4.2 Irradiance data generation

Solar data are obtained using the GIS-based infrastructure of [1]. Input GIS data are expressed through a *Digital Surface Model* (DSM), which is a high-resolution raster image representing terrain elevation of the building of interest. The DSM allows to recognize obstacles over the surface (e.g. chimneys) and to estimate the evolution of shadows over time, with 15-minute temporal resolution. The overall trace over time is then obtained by combining weather data, retrieved from weather stations, along with the shadow model.

4.3 Experimental setup

We applied the proposed PV module placement algorithm to the lean-to roofs of two industrial buildings. The roofs face S-S/W with inclination of 26^o; the first is of 4m×6m, and the second is of 4m×12m. The key features of each roof are reported in Table 1. Simulations cover one year, from March 2010 to February 2011. Figure 3 shows the 75th percentile of irradiance distribution of the two roofs (brighter colors represent higher irradiance). Irradiance is quite non uniform, as an effect of both roof orientation and of the presence of surrounding encumbrances.

4.4 Simulation results

4.4.1 Execution time. We implemented all algorithms in MATLAB (R2017a). The execution time of the placement is proportional to the number of cells, and it required less than 1.5s for each roof on an Intel 8-core i7 server with 15.4GB of RAM. On average, 16% of the execution time is devoted to the application of the Hungarian algorithm, while about 66% of CPU time is used for the topology construction. This proves the feasibility of the tiling problem, despite of its theoretical complexity.

4.4.2 Generated layout. Figure 3 compares the traditional portrait and landscape placements with the irradiance-driven tiling returned by our algorithm. Colored rectangles represent panels, with panels of the same color belonging to the same series string. The portrait and landscape configurations follow the typical topology: all panels positioned with the same orientation, and nearby panels connected in series. Vice versa, the proposed algorithm places the panels so that irradiance distribution over time is maximized. As a result, both the orientation of the PV modules and their topology reflect the irradiance distributions on the roofs: in the first roof, the least irradiated area is covered by panels connected in series (in blue). Vice versa, in the second roof, the most irradiated area is covered with panels in series, oriented by following the irradiance distribution pattern (purple and green).

4.4.3 Generated power. Table 1 reports the corresponding power production of the two roofs for all configurations. The table shows that the proposed solution can significantly improve energy production on a yearly basis, with improvements that range from 12% to 42%. Obviously, the magnitude of benefit is constrained by the available space, as all solutions occupy the entire roof. However, the numbers show that a more careful orientation and connection of panels can lead to sensible improvements.
Both roofs clearly prove the effectiveness of the adopted irradiance-based topology: the traditional placements have similar topologies, as they put in series the same areas of the roof. The more irregular topology applied by the proposed algorithm (and highlighted by Figure 3) increases the power production by better matching the variance in irradiance on the surface.
Additionally, roof 1 highlights also the advantage of the proposed hybrid orientation, that explains the huge difference in terms of power production between the traditional placements. Roof 1 is indeed characterized by a very heterogeneous distribution of irradiance (Figure 3-(a)): thus, an irradiance-agnostic orientation might place a PV module across two cells that are mismatched in terms of irradiance, thus reducing the possible power production.

Table 1: Characteristics of each roof and power production of the configurations in Figure 3.

Roof	W×H	Panels (#)	Panels Series	PV panel model	PV system production: Portrait MWh	Landscape MWh	Proposed algorithm MWh	Proposed algorithm w.r.t. portrait	Proposed algorithm w.r.t. landscape	Proposed algorithm Time (s)
1	8×12	48	12	Proposed	5.811	4.614	6.575	+13.15%	+42.51%	0.664
				[12]	5.917	4.743	6.678	+12.85%	+40.81%	0.801
2	8×24	96	16	Proposed	17.107	17.118	20.391	+19.20%	+19.12%	1.438
				[12]	18.044	18.056	21.526	+19.30%	+19.22%	1.595

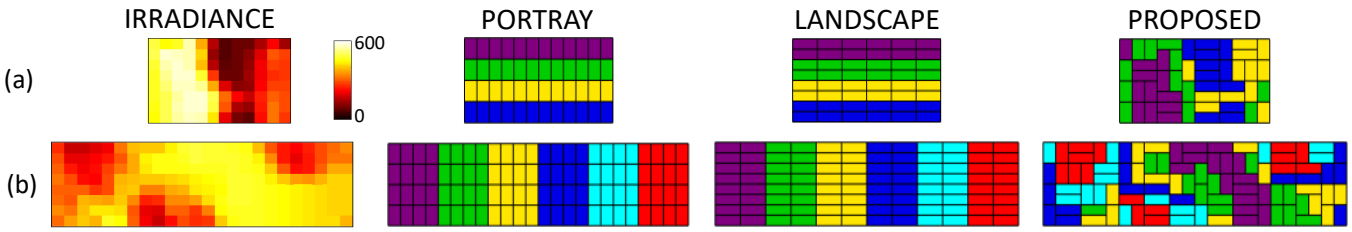

Figure 3: Irradiance distribution over the roofs $[W/cm^2]$ and comparison of three placements: traditional portrait and landscape orientation and result of the proposed algorithm. Rectangles with the same color represent panels connected in series.

4.4.4 Extensibility to other PV module models. To confirm the extensibility of the proposed approach, we applied the placement algorithm to a more complex model built for the same PV module. The model, presented in [12], considers also the effect of temperature on power production, thus gaining a more accurate estimation. Table 1 reports the corresponding power production for the same roof configurations: the results prove that the placement algorithm can be applied also to this more complex model, at the expense of slightly longer simulation times (that are still below 1.6s in all configurations). The difference in terms of power production (in average 3.61%) lies in the different power model. However, the proportion between the configurations is almost identical across the two models.

4.4.5 Wiring costs. The proposed irregular placement will slightly increase the wiring resources, and therefore cost and possibly power. However, a quick analysis of the latter shows that these penalties are marginal. Firstly, since the surface area is a constant, the difference between the total cable length is moderate; Figure 3 shows that an individual series string can indeed be distributed over the entire surface, but some spatial vicinity between blocks of the string is still maintained.
Concerning cost, a typical AWG 10 cable has an approximate cost of $1\$/m$, so, even with 10-20 meters of extra cables the cost overhead would be negligible compared to the cost of the energy increase (avg. 20.14GW). Power overhead is also minimal: the AWG 10 resistive loss is $\approx 7m\Omega/m$; assuming a 4A current in a series string (corresponding to an irradiance of $600W/cm^2$), the power loss is $RI^2 \approx 0.11W/m$, i.e., $\approx 0.5kW/m$ of energy per string in one year (assuming 50% of the time at zero current for dark periods). Multiplying by the number of strings and comparing to the numbers of Table 1, the overhead is below 0.1%.

5 CONCLUSIONS

This work proposed an irradiance-based placement algorithm for PV panels, that sensibly increases power production over a roof tiled with PV modules. The proposed solution exploits two degrees of freedom, namely, PV module orientation and the topology of the overall panel, to match the variance in irradiance on the surface and minimize the effects of shading. We demonstrated the application of the method to two real world case studies, showing an energy increase as much as 12-42% larger than traditional PV installations.

REFERENCES

[1] L. Bottaccioli, E. Patti, E. Macii, and A. Acquaviva. GIS-based software infrastructure to model PV generation in fine-grained spatio-temporal domain. *IEEE Systems Journal*, pages 1--10, 2017.
[2] L. de Sousa, C. Eykamp, U. Leopold, O. Baume, and C. Braun. iGUESS - a web based system integrating urban energy planning and assessment modelling for multi-scale spatial decision making. In *iEMSs 2012*, pages 1--8, 2012.
[3] M. Electric. PV-MF165EB3 datasheet. https://www.mitsubishielectricsolar.com/images/uploads/documents/specs/L-175-4-B6504-A_MF165EB3.pdf.
[4] energysage. What is the average solar panel size and weight? http://news.energysage.com/average-solar-panel-size-weight.
[5] S. Freitas, C. Catita, P. Redweik, and M. Brito. Modelling solar potential in the urban environment: State-of-the-art review. *Renew. Sustainable Energy Rev.*, 41:915--931, 2015.
[6] D. Klarner and J. Pollack. Domino tilings of rectangles with fixed width. *Discrete Mathematics*, 32(1):45--52, 1980.
[7] Mapdwell Solar System. http://www.mapdwell.com.
[8] C. Radin. Space tilings and substitutions. *Geometriae Dedicata*, 55(3):257--264, 1995.
[9] B. Resch, G. Sagl, T. Törnros, A. Bachmaier, J.-B. Eggers, S. Herkel, S. Narmsara, and H. Gündra. GIS-based planning and modeling for renewable energy: Challenges and future research avenues. *ISPRS IJGI*, 3(2):662--692, 2014.
[10] S. Suri. *Bipartite matching & the Hungarian method.*
[11] Y. Tsuno, Y. Hishikawa, and K. Kurokawa. Temperature and irradiance dependence of the I-V curves of various kinds of solar cells. *Proc. of PVSEC*, pages 422--423, 2005.
[12] S. Vinco, L. Bottaccioli, E. Patti, A. Acquaviva, E. Macii, and M. Poncino. GIS-based optimal photovoltaic panel floorplanning for residential installations. *Proc. of IEEE Design, Automation and Test in Europe (DATE)*, pages 1--6, 2018.
[13] S. Vinco, Y. Chen, E. Macii, and M. Poncino. A unified model of power sources for the simulation of electrical energy systems. In *Proc. of ACM/IEEE GLSVLSI*, pages 281--286, 2016.
[14] S. Vinco, A. Sassone, M. Poncino, E. Macii, G. Gangemi, and R. Canegallo. *Modeling and Simulation of the Power Flow in Smart Systems.* Springer, 2016.
[15] T. Voegtle, E. Steinle, and D. Tovari. Airborne laserscanning data for determination of suitable areas for photovoltaics. *ISPRS LS*, pages 215--220, 2005.